Galician medical journal 2024
Vol. 31, Issue 1, e-GMJ2024-A01
DOI: 10.21802/e-GMJ2024-A01

Case Report | **Pathology**

Multiple Myeloma Patient with Secondary Liver and Tongue Involvement, Complicated by COVID-19-Induced ARDS: An Autopsy Case Report and Literature Review

Viktoriya Matskevych[1*], Khrystyna Ilnytska[1], Tetiana Lenchuk[1], Yulian Mytsyk[2], Elvira Kindrativ[3], Nataliia Hlushko[4]

Abstract

Background. Liver involvement secondary to multiple myeloma is a rare and uncommon radiologic finding. Such extraosseous secondary lesions as well as tongue involvement require pathohistological confirmation to prevent misdiagnosis. Clinical and laboratory diagnostics are challenging in patients with COVID-19 and underlying multiple myeloma and its secondary lesions, leading to difficulties in treatment and outcomes.

Case Report. A 64-year-old male patient, not vaccinated against COVID-19, with a history of multiple myeloma presented with symptoms of headache, fatigue, dyspnea, cough, and fever. The patient's medical history was intricate, involving cholecystectomy and a diagnosis of multiple myeloma, which was subsequently treated with chemotherapy and radiation therapy. Additionally, uncommon liver and tongue involvement secondary to multiple myeloma was found. Upon admission, the patient's peripheral oxygen saturation was 90%, accompanied by increasing shortness of breath and a respiratory rate of 26 breaths per minute. A positive COVID-19 test was recorded. A lung computed tomography revealed bilateral multifocal areas of ground-glass opacity and consolidation, encompassing the entire pulmonary regions, corresponding to CO-RADS 6. The patient was admitted to the intensive care unit. Despite initiating oxygen support and symptomatic therapy, the patient's death occurred. Autopsy confirmed the development of severe acute respiratory distress syndrome and bilateral hemorrhagic pneumonia, with multiple myeloma as a contributing factor.

Conclusions. This case report highlighted the rare occurrence of secondary liver involvement in multiple myeloma, characterized by nodules with distinct imaging features. It underscored the importance of identifying coexisting lesions, such as tongue involvement, and the diagnostic challenges they pose. Additionally, the case emphasized the need for comprehensive clinical assessment in patients with concurrent COVID-19 and underlying multiple myeloma, as it may lead to the development of acute respiratory distress syndrome.

Keywords

2019 Novel Coronavirus Disease; Multiple Myeloma; Liver Involvement; Acute Respiratory Distress Syndrome; Computed Tomography; Diffuse Alveolar Damage

[1] 1Department of Radiology and Radiation Medicine, Ivano-Frankivsk National Medical University, Ivano-Frankivsk, Ukraine
[2] Department of Radiology and Radiation Medicine, Danylo Halytsky Lviv National Medical University, Lviv, Ukraine
[3] Department of Pathological Anatomy, Ivano-Frankivsk National Medical University, Ivano-Frankivsk, Ukraine
[4] Department of Hematology, "Regional Clinical Hospital of Ivano-Frankivsk Regional Council", Ivano-Frankivsk, Ukraine
*__Corresponding author__: vmatskevych@ifnmu.edu.ua

Publication history:
Received: July 7, 2023
Revisions Requested: August 15, 2023
Revision Received: October 8, 2023
Accepted: October 17, 2023
Published Online: January 8, 2024

Introduction

The difficulty in diagnosing multiple myeloma (MM) lies in the challenge of identifying secondary extraosseous lesions with the currently available radiological techniques [1]. Combining methods and techniques employed in radiology and pathology with monitoring blood and urine changes raises the accurate diagnosis of atypical MM spreading [2]. It is important for radiologists to be more aware of rare locations of MM metastasis as they are the first to face the visualization of such lifetime changes [3]. The COVID-19 pandemic has posed an additional challenge for all diagnostic specialties [4]. This includes various visual, laboratory, and morphological findings that need differentiation in patients with hematological malignancies diagnosed with severe acute respiratory syndrome coronavirus 2 (SARS-CoV-2) [5]. Individuals with hematologic malignancies are considered to have a higher susceptibility to SARS-CoV-2 infection and be at increased risk of fatality due to the presence of an underlying lymphoproliferative disease, treatment-induced immunosuppression, or comorbidities [6, 7]. A meta-analysis by Yang L *et al.* revealed that cancer is an independent risk factor for mortality in COVID-19 patients [8]. Moreover, the presence of malignancy has been identified as one of the key contributing factors impacting the mortality pattern in patients with ischemic heart disease, hypertension, and diabetes mellitus [9]. Additionally, anemia, which is commonly present in patients with bone marrow cancer, serves as risk determinant of severe COVID-19 outcomes [10–12]. Furthermore, in MM patients, adverse prognostic indicators, in addition to the above mentioned, are more lines of therapy, older age, and CD38 antibody-directed and B-cell maturation antigen-directed therapies [13]. We present a case report of secondary liver nodular and tongue involvement in MM patient with COVID-induced acute respiratory distress syndrome (ARDS).

Case Report

Patient Information

Primary Concerns and Symptoms

On November 18, 2022, a 64-year-old male patient was admitted to the hospital presenting with complaints of persistent headache, fatigue, dyspnea, cough, and fever, which were unresponsive to antipyretic medication administered at home. The patient had been experiencing these symptoms for five days, during which his condition progressively worsened. He attributed his deteriorating condition to his underlying illness. However, when his wife began experiencing similar symptoms, he sought medical assistance at the hospital.

Medical History

The patient's medical history indicated cholecystectomy performed in 2020 and negative test results for human immunodeficiency virus (HIV), hepatitis B virus (HBV), and hepatitis C virus (HCV). On December 2, 2021, a year to the current hospitalization, the patient consulted a vertebrologist due to complaints of back pain. The patient's neuroorthopedic status was characterized by difficulty walking due to pain, increased thoracic kyphosis, and tense paravertebral muscles in the thoracic region. The spinous processes, intervertebral spaces, and paravertebral points from Th II to Th XII were tender upon palpation. Peripheral lymph nodes were not palpable. Computed tomography (CT) imaging revealed a pattern of metastatic lesions in the thoracic spine and pelvic bones. Magnetic resonance imaging (MRI) demonstrated signs of infiltrative changes in the bone marrow of the Th IX vertebra complicated by spinal canal stenosis. Additional infiltration foci were visualized in the bodies of the Th III, Th VII, Th VIII vertebrae, in the left pedicle of the Th III arch vertebra, in the XII left rib, and in both iliac bones. Subsequently, open biopsy of the Th IX vertebra was carried out for morphological examination. Routine histological analysis revealed tissue fragments measuring 0.3-0.5 cm and consisting of white fragile material and two fragments of dense bone measuring 0.5 cm. Microscopically, diffuse proliferations of large, rounded lymphoid and plasmacytoid cells were observed among the fragments of compact and cancellous bone, morphologically corresponding to plasmacytoma. Immunohistochemical investigation (Fig. 1, 2) revealed a positive reaction of tumor cells with CD38 Ab-3, CD79 alpha, CD138, CD56/NCAM-1, and Kappa light chain ab-2. Conversely, CD20, Cytokeratin, Pan Ab-1, SOX-10, and Lambda light chain ab-2 exhibited a negative reaction with tumor cells. The immunophenotype and morphology of the tumor were indicative of predominantly pleomorphic and immature cells, supporting a diagnosis of plasmacytoma (Fig. 1, 2).

Diagnosis. C90.0 - stage 1 multiple myeloma (International Staging System), with prominent osteolytic syndrome, secondary involvement of the Th IX-X vertebrae, resulting in significant pain. Frankel grade E spinal cord compression, accompanied by multiple affected iliac bones, spine, and XI left rib.

Coexisting Conditions. Chronic ischemic heart disease (I25.8).

Treatment. The patient received long-term treatment for heart disease with bisoprolol, ivabradine, and acidum acetylsalicylicum, administered from January 12, 2022, to September 17, 2022, along with five courses of chemotherapy using the bortezomib, cyclophosphamide, and dexamethasone (VCD) protocol, followed by two courses of chemotherapy according to the bortezomib, lenalidomide, and dexamethasone (VRD) protocol. Subsequently, a chemotherapy course involving pomalidomide, dexamethasone, and bortezomib was administered, during which patient's condition worsened and back pain increased. Additionally, the patient underwent radiation therapy for the thoracic spine, with a total dose of 30 Gray administered.

Outcomes. The bone marrow sample exhibited the following altered indices: metamyelocytes - 4% (Normal (N) - 8-15%), segmented neutrophils - 25.5% (N - 13.1-24.1%), monocytes - 5% (N - 0.7-3.1%), lymphocytes - 16% (N - 4.3-13.7%), and a mitosis of the erythroid cell line ratio of 1:500 (N - 3:500).

After the completion of treatment and relative stabilization of the clinical condition and laboratory parame-

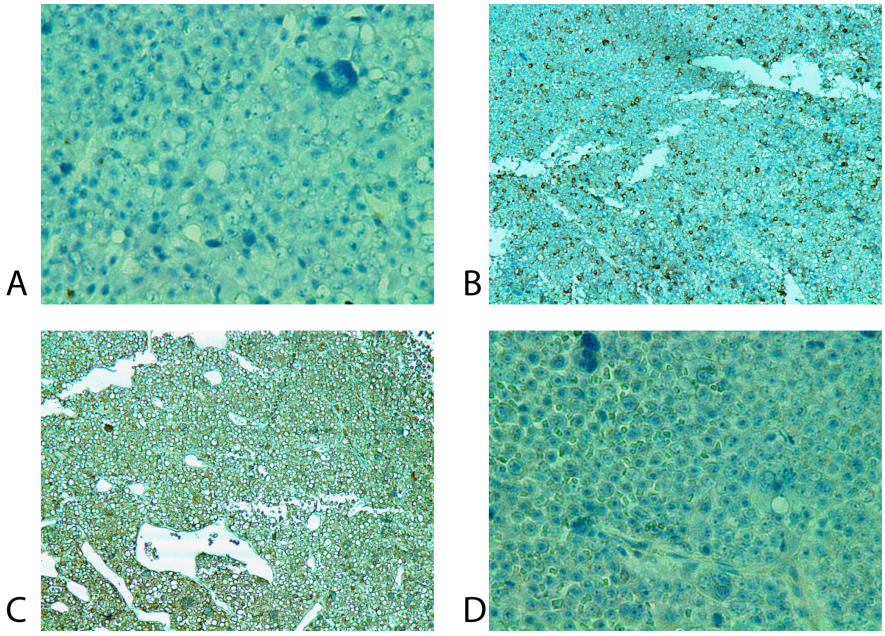

Figure 1. Immunohistochemistry of secondary myeloma lesion of the Th IX vertebra: **A)** CD 20 (Ab-1, Thermo Scientific), magnification - ×400; **B)** CD 79 alpha (SP18, Thermo Scientific), magnification - ×100; **C)** Kappa light chain ab-2 (Rabbit polyclonal, Thermo Scientific), magnification - ×100; **D)** Cytokeratin, Pan Ab-1 (AE1/AE3), Thermo Scientific), magnification - ×400.

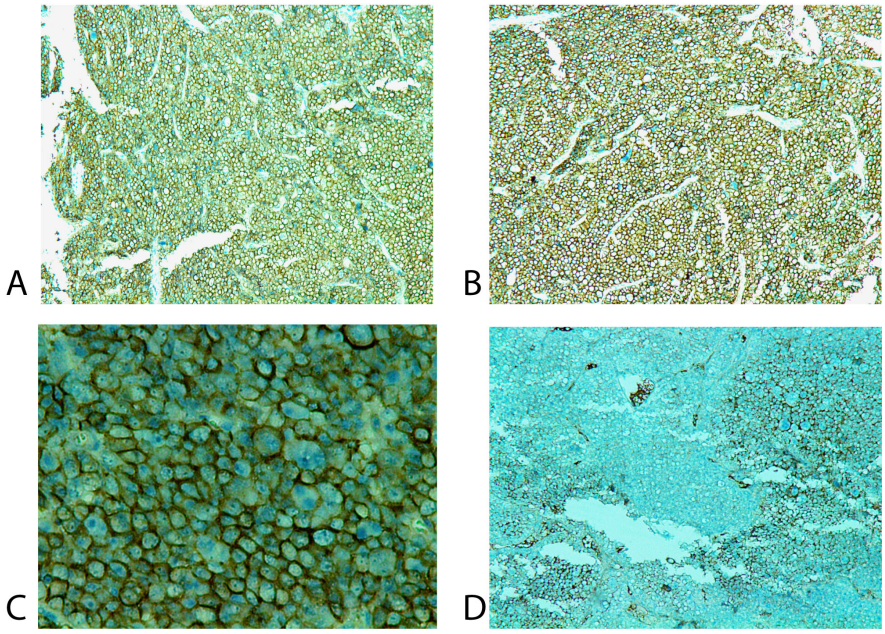

Figure 2. Immunohistochemistry of secondary myeloma lesion of Th IX vertebra: **A)** CD 38 Ab-3 (Clone 38C03, NeoMarkers), magnification - ×100; **B)** CD 56/NCAM-1 (Clone 123C3, Master Diagnostica), magnification - ×100; **C)** CD 138 (EP201, Master Diagnostica), magnification - ×400; **D)** Lambda light chain ab-2 (Rabbit polyclonal, Thermo Scientific), magnification - ×100.

ters (Table 1), the patient was discharged home. During a short two-week stay from September 18, 2022, to October 3, 2022, the patient developed fever, weakness, and weight loss. Upon readmission to the hospital on October 4, 2022, and subsequent ultrasound examination, multiple liver lesions were detected. These lesions appeared as round hypo- and hyperechoic lesions measuring 0.8-1.4 cm, as confirmed by contrast-enhanced abdominal CT scan, where the lesions were hypodense in the venous phase (Fig. 3). Furthermore, the presence of atypical plasma cells was confirmed through liver biopsy with immunohistochemical analysis. Additionally, ultrasound examination revealed effusion in both pleural sinuses, with hemorrhagic content during puncture.

Additionally, during the examination, a mass was found within the root of the tongue: a mixed growth tumor of

Table 1. Progression of laboratory results over time.

Laboratory indices	Disease stage description					Reference interval
	Secondary spinal lesions (Dec 2, 2021)	After chemotherapy and radiation therapy treatment (Sep 15, 2022)	Secondary root of the tongue and liver lesions (Oct 24, 2022)	COVID-19 (Nov 18, 2022)	COVID-19 (Nov 21, 2022)	
Complete blood count test						
White blood cells (x$10^9/\mu$L)	7.16	8.47	2.96	4.81	9.3	4.0-9.0
Segmented neutrophils (%)	82	77	64	68	82	47-72
Band neutrophils (%)	2	2	25	20	2	1-6
Lymphocytes (%)	12	11	8	8	12	19-37
Neutrophil-to-lymphocyte ratio	7	7.18	11.12	11	7	0.78-3.0
Monocytes (%)	3	10	0	2	3	3-11
Eosinophils (%)	1	0	0	2	1	0.5-5
Basophils (%)	0	0	3	0	0	0-1.5
Platelets (x$10^9/\mu$L)	145	229	35	145	130	150-350
Red blood cells (x$10^{12}/\mu$L)	4.4	4	3.8	2.8	2.4	4.7-6.1
Haemoglobin (g/L)	130	108	105	94	71	130-170
Haematocrit (L/L)	0.38	0.33	0.29	0.27	0.22	0.4-0.5
Erythrocyte sedimentation rate (mm/hour)	27	33	41	45	72	1-10
Serum biochemistry panel						
Glucose (mmol/L)	5.96	5.74	5.42	6.31	6.71	4.2-6.4
Total protein (g/L)	76	65.9	55.7	64	69	66-87
Total bilirubin (μmol/L)	9.1	10.5	24.7	14.7	8	5-21
Direct bilirubin (μmol/L)	1.7	2.6	6.5	2.7	1.3	≤ 5.1
Aspartate aminotransferase (U/L)	21.8	32	94.1	15.8	24.3	<37
Alanine aminotransferase (U/L)	52	27.8	38.3	13.2	31.9	<41
Urea (mmol/L)	7.84	6.75	8.81	16.4	27.3	≤ 8.3
Creatinine (μmol/L)	125.7	115	169.5	226.3	341.9	62-115
Potassium (mmol/L)	4.44	3.58	4.38	4.19	6.1	3.44-5.3
Sodium (mmol/L)	141.1	131	131.2	125.3	133.2	130.5-156.6
Chlorides (mmol/L)	99.5	101.5	109.1	104.8	105.9	95-110
Total calcium (mmol/L)	n/p	n/p	2.98	n/p	n/p	2.15-2.50
Procalcitonin (ng/ml)	<0.1	n/p	n/p	<0.1	0.43	<0.5
Coagulation panel						
Prothrombin time test (s)	14.1	15.3	15.7	10.7	12.4	10.5-14.8
Prothrombin index (%)	92.9	83.6	81.5	103.5	88.8	85.4-121.6
Quick prothrombin time test (%)	68.6	64.3	60.8	77.2	66.1	80-120
International normalized ratio	1.16	1.24	1.28	0.97	1.13	0.8-1.2
Fibrinogen (g/L)	3.15	3.88	4.7	4	4.4	2-4
Blood plasma protein fractions (electrophoresis method)						
Albumin (g/L)	49.31	31.55	26.17	n/p	n/p	34.4-45.0
α1-globulin (g/L)	3.14	1.53	2.9	n/p	n/p	1.6-6.7
α2-globulin (g/L)	10.52	6	11	n/p	n/p	5.6-12.4
β-globulin (g/L)	22.87	9.9	3.92	n/p	n/p	4.4-11.6
β2-microglobulin (g/L)	2.1	1.9	n/p	n/p	n/p	0-3.0
γ-globulin (g/L)	14.16	5.99	9.34	n/p	n/p	5.5-13.4
Monoclonal serum protein IgA Kappa in the gamma region (g/L)	4.37	Absent	1.64	n/p	n/p	Absence
Urine plasma protein fractions (electrophoresis method)						
Bence-Jones protein of Kappa class in the beta region (g/L)	0.737	0.035	0.157	n/p	n/p	Absence

Notes: n/p – analysis was not performed.

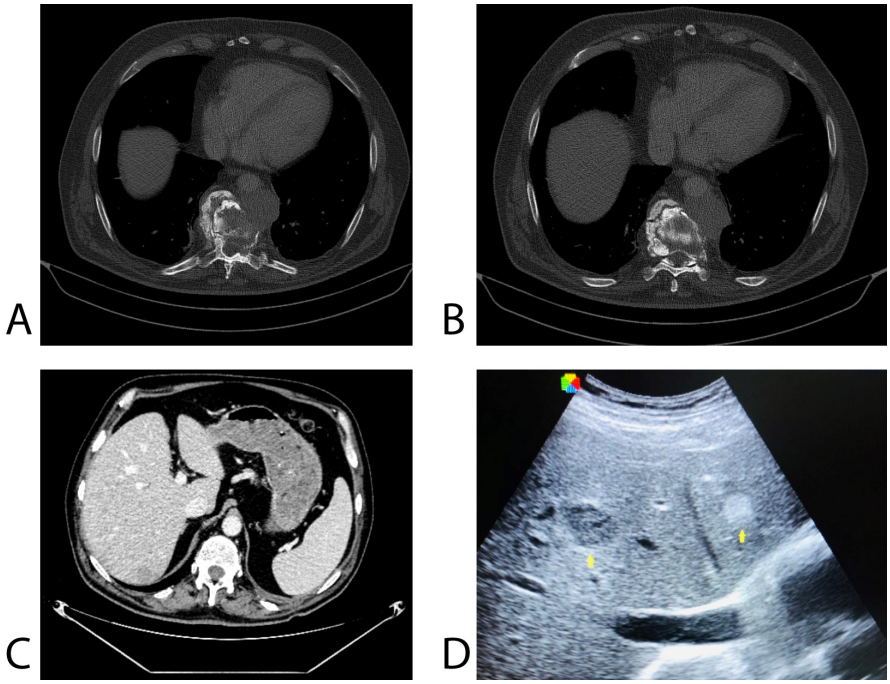

Figure 3. Imaging findings of lesions secondary to multiple myeloma: **A, B)** CT signs of destructive osteolytic foci with cortical layer disruption and a paravertebral pathologic soft tissue mass; **C)** CT signs of subcapsular liver hypodense lesion in the right hepatic lobe (S7) in the venous phase; **D)** Ultrasound findings of multiple hypoechogenic and hyperechogenic lesions in the liver.

2.5 to 3.0 cm located closer to the right edge of the lingual tonsil. The mucous membrane above it appeared slightly infiltrated and pale bluish. Pathohistological investigation revealed infiltration by atypical plasma cells and necrotic debris at the periphery of the sections (Fig. 4), which was further confirmed by immunohistochemical analysis.

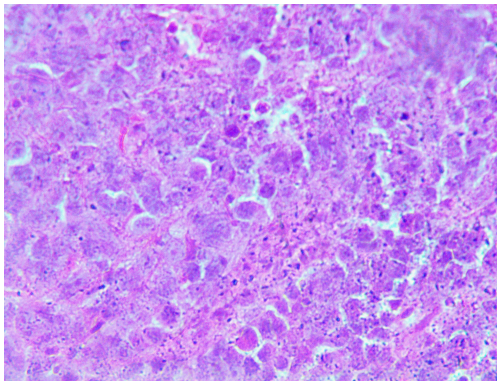

Figure 4. Root of the tongue: lesion secondary to multiple myeloma. Extensive infiltration of fibrous tissue by atypical plasma cells. Hematoxylin and eosin staining, magnification - $\times$400.

Considering the patient's complaints, radiological and pathohistological patterns, clinical and laboratory findings as of October 24, 2022 (Table 1), the patient was prescribed dexamethasone and denosumab for hypercalcemia (total calcium 2.98 mmol/L) and massive osteolytic lesions of the skeleton. Platelet transfusion performed due to thrombocytopenia (platelets 35 x $10^9/\mu$L). Peripheral lymph nodes were not palpable. No hemorrhagic syndrome was found. Radiation dermatitis resulted in hyperpigmentation of the skin over the thoracic spine region. Vesicular lung sounds were heard. Ultrasound examination revealed a free left pleural sinus and 1 cm of liquid content in the right sinus. The arterial blood pressure was 120/75 mmHg and the pulse rate was 82 beats per minute. The abdomen appeared soft and non-tender upon palpation. The liver was non-tender with a rounded edge, palpable 2 cm below the costal margin. The spleen was not palpable. Heart sounds were rhythmic and clear. No signs of edema and urinary hesitancy were found. No bacterial growth in blood culture was detected. Fever was managed with a daily dose of diclofenac and analgin. After stabilization of the condition during a three-week hospitalization period (from the 4th to the 26th of October 2022), the patient was discharged home under family physician care. Three weeks after staying at home and having a contact with a family member who had COVID-19, the patient developed symptoms of acute viral illness (November 18, 2022), specifically fever, cough, shortness of breath, headache, and increasing fatigue.

Clinical Findings and Diagnostic Assessment

The patient was admitted to the intensive care unit due to his peripheral oxygen saturation at rest being 90%, increasing shortness of breath, a respiratory rate of 26 breaths per minute, and a positive rapid COVID-19 test (followed by positive RT-PCR). The patient was not vaccinated against COVID-19. CT lung examination revealed bilateral multifocal areas of ground-glass opacity and consolidation throughout the pulmonary parenchyma, corresponding to

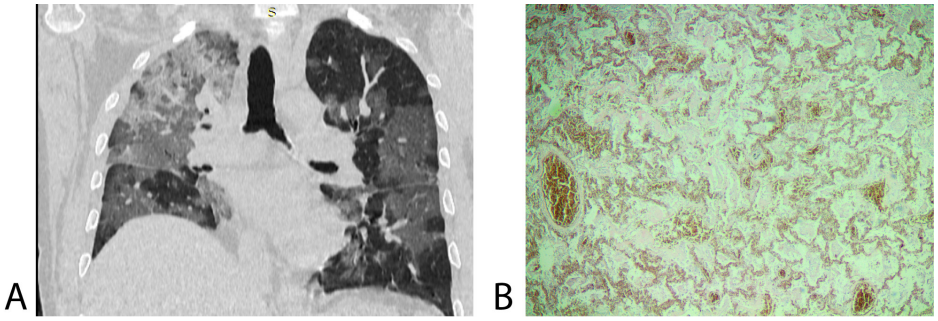

Figure 5. COVID-19 lung findings: **A)** Coronal reconstruction of CT scan: bilateral diffuse ground-glass opacity with consolidation and fibrous bands; **B)** Postmortem histological pattern (hematoxylin and eosin-stained section; magnification - ×40: lung tissue with diffuse alveolar damage, swelling of the alveolar septa with luminal filling by exudate, desquamation of alveolocytes, stasis and the initial development of the microcirculatory intravascular thrombosis.

CO-RADS 6 (Fig. 5A) according to the CO-RADS classification initiated and standardized by the COVID working group of the Dutch Radiological Society [14].

Treatment

The patient has been prescribed antipyretic medication and dexamethasone. Due to the patient's dyspnea and decreased peripheral oxygen saturation, oxygen support was initiated with facial mask. Later, to improve efficiency, it was replaced with the Continuous Positive Airway Pressure (CPAP) oxygen therapy system. Since the patient's clinical condition, along with lab panel (Table 1), continued to deteriorate, a clinical team decided to initiate invasive mechanical ventilation in volume-controlled synchronized intermittent mandatory ventilation (VC-SIMV) mode. Clinical death, however, occurred in one day. Despite resuscitation efforts, the patient could not be revived, and the patient was pronounced biologically dead on November 22, 2022, at 12.50 p.m.) An autopsy was conducted in the Department of Pathology to determine the specific cause of death. The overall hospitalization period due to COVID-19 was five days.

Fig. 6 depicts the sequence and chronology of patient's events to briefly describe his history.

Outcome (a brief overview of autopsy protocol concerning diseases)

Areas of bone destruction in Th III, Th VII - Th IX were revealed during macroscopic examination at autopsy. The pleural cavities contained a small amount of bloody fluid. The root of the tongue exhibited a whitish tumor-like mass measuring 2.5 to 3.0 cm. The mucous membranes of the trachea and main bronchi appeared swollen, plethoric, and were covered with semi-liquid hemorrhagic mucus. Upon cutting the lungs, variegated areas of reddish consolidation were observed. The lung section revealed a moderate presence of frothy bloody fluid. The bronchial walls showed no signs of thickening. Semi-liquid hemorrhagic mucus was present within the bronchi lumen. The liver appeared enlarged, brown, with whitish multiple foci lacking clear contours up to 13 mm in diameter with a dense structure. The gall bladder was absent. The kidney tissue appeared pale pink with corticomedullary differentiation. The spleen exhibited a soft texture, and the scraping was prominent. The inner plate of the skull displayed multiple bone round defects with a diameter of up to 0.4 cm. The dura mater of the brain was tense, plethoric, while the pia mater was moderately gelatinous.

During microscopic histological examination, the tissue of the root of the tongue exhibited atypical plasma cell infiltration. In the liver, perisinusoidal spaces focalized the presence of erythrocytes and atypical plasma cells. Large foci of atypical plasma cells were observed within the connective tissue surrounding the liver, without visualization of the capsule. The kidneys displayed focal necrosis of the epithelium of convoluted tubules, with widened tubule lumens containing homogeneous pink content. Blood vessels were plethoric.

The lung tissue exhibited diffuse alveolar damage characterized by cellular fibromyxoid exudates. Desquamation of alveolocytes with the formation of hyaline membranes was visualized. Interstitial mononuclear inflammatory infiltrates, primarily composed of lymphocytes, were present,

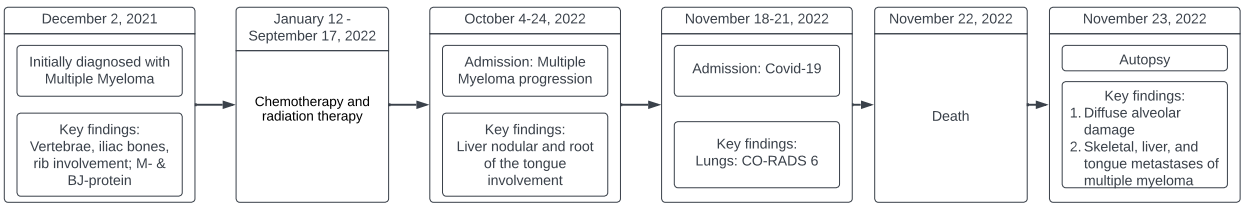

Figure 6. Timeline: from initial multiple myeloma diagnosis to fatal ARDS complication from COVID-19.

along with multiple hemorrhages and microthrombosis in the circulatory system (Fig. 5B). The postmortem biomaterial collected from the trachea, bronchi, and lungs tested positive for COVID-19 using RT-PCR, a result consistent with the antemortem test performed at the intensive care unit. Additionally, Candida albicans was detected by microbiologic method in the postmortem tissues of the trachea and bronchi.

Autopsy summary

Underlying autopsy diseases: 1) U07.1 – 2019-novel coronavirus acute respiratory disease. 2) C90.0 – Multiple Myeloma (according to clinical and autopsy data). *Main disease complications:* J12.8 – Bilateral hemorrhagic pneumonia. J96 – Respiratory failure. N19 – Kidney failure (necrosis of the epithelium of convoluted tubules). G93.9 – Disorder of brain. J81 – Pulmonary edema. G93.6 – Cerebral edema. J80 – Acute respiratory distress syndrome. J91 – Serous-hemorrhagic bilateral pleural effusion. C78.7 – Secondary malignant neoplasm of liver. C79.89 – Secondary malignant neoplasm of root of the tongue. R16.1 – Splenomegaly. *Coexisting diseases:* I25.8 – Chronic ischemic heart disease.

Cause of death

I. Directly caused the death: Acute respiratory distress syndrome, bilateral hemorrhagic pneumonia, COVID-19. II. Other significant conditions contributing to death, but not resulting in the underlying cause: Multiple myeloma.

Discussion

A distinctive feature of this case is the manifestation of liver involvement secondary to MM. Remarkably, the identification of hepatic invasion by MM during radiological examination is an infrequent occurrence. Sonography revealed round hypo- and hyperechoic lesions, while contrast-enhanced abdominal CT scans indicated hypodense lesions in the venous phase. Our case report correlates with nodular liver lesions involving MM where CT findings where biopsy confirmed [15]. Oshima *et al.* have reported a 28.8 % incidence of secondary hepatic extraosseous involvement at autopsy. This prevalence is attributed to the predominant diffuse infiltration of the liver by plasma cells, a feature that often necessitates microscopic examination for detection. The formation of visible, well-defined tumor nodules, detectable through radiological methods, is extremely rare in this context [16]. Heckmann *et al.* reported that radiologic evidence of extramedullary hepatic involvement by plasmacytoma was predominantly limited and described it as hypo- or hyperechoic solitary or multiple lesions on ultrasound and hypodense with little or no contrast enhancement on CT, scan which correlates with radiologic findings observed in the present case [17]. A rare nodular lesion of the liver with MM was evidenced by nine (0.35%) cases of macroscopic imaging among 2,584 patients [18]. Kwok *et al.* described two cases of secondary MM involvement of the liver, in which bilobar hypo- and hyperechoic lesions (the latter occasionally with hypoechoic rims) were detected [19], resembling the sonographic pattern presented in our case report. Therefore, the visual radiologic features of hepatic MM involvement are not clearly specific and may differ, posing a challenge in distinguishing it from other liver lesions, especially in cases with an atypical clinical presentation. In a systematic review and meta-analysis, Lu *et al.* found very high sensitivity and specificity (96% and 77.8%, respectively) of positron emission tomography-computed tomography (PET/CT) in detecting secondary extramedullary involvement by myeloma [20]. Prospective and retrospective studies have, however, established that whole-body diffusion-weighted (DWI) MRI is more sensitive than PET/CT in detecting the original tumor size and assessing treatment outcomes based on the updated International Myeloma Working Group (IMWG) criteria [21]. Moreover, a meta-analysis conducted in 2018 found that whole-body MRI was less specific than fluorodeoxyglucose-positron emission tomography (FDG PET/CT) in staging this bone marrow cancer [22]. A lower specificity of whole-body MRI may be due to its ability to detect nonviable lesions, while FDG PET/CT reveals glucose metabolism in viable cells [23]. To address the challenge of distinguishing nonviable lesions from viable ones with conventional MRI sequences, the use of functional imaging techniques such as DWI for response assessment has been explored [24]. Additionally, a reported case demonstrated hyperintense lesions with bilobar distribution in the liver parenchyma identified through MRI [25]. This method is considered as the most accurate imaging technique for the initial diagnosis of MM [26]. For the diagnostic assessment of the present case, contrast-enhanced CT of the chest, abdomen and pelvis, MRI of the spine and pelvic skeleton, bone marrow sampling, and biopsy of the thoracic vertebra were performed. The phenotype of plasma cells was then determined using immunohistochemistry on paraffin-embedded sections. Additionally, monoclonal immunoglobulin A (IgA) -kappa protein in the serum and Bence-Jones (kappa-type) protein in urine were measured. On readmission (October 2022), secondary liver and root of the tongue involvement, confirmed by biopsy, (CT hypodense and ultrasound hypo- and hyperechogenic lesions) were identified. Therefore, the aforementioned criteria were sufficient for establishing MM diagnosis according to the IMWG criteria [27] and a PET/CT scan was not performed in this case.

It is important to differentiate between secondary lesion of the tongue by multiple myeloma and extramedullary plasmacytoma of the tongue which manifests itself in the tongue tissue and can progress to MM in 10-40% of patients [28–30]. In the demonstrated clinical episode, we report the concurrent detection of a secondary lesion in the root of the tongue originating from primary bone localization, which was identified alongside secondary liver involvement.

It is crucial to highlight that due to the controversial and ambiguous radiological presentation of MM manifestations, biopsy samples followed by immunohistochemical staining with phenotype determination are imperative for accurate diagnosis and subsequent treatment [31]. In this case, biopsy of the thoracic vertebra (MM manifestations in December 2021) following immunohistochemistry

with immunophenotype determination were performed after CT and MRI imaging. Additionally, biopsy-confirmed liver and root of the tongue involvement were identified on sonography and CT, respectively. Subsequently, postmortem macro- and microscopic morphological diagnostics were carried out. The common morphological pattern of pathologically altered areas in the vertebra, liver, and root of the tongue, characterized by atypical plasma cells, was identified through routine and immunohistochemistry stainings. Histologic diagnostics, complemented by immunohistochemical staining of tissue samples, serves as the cornerstone for diagnosing MM, as well as other lymphoproliferative disorders. This approach allows for the characterization of cellular structures, with particular emphasis on determining the phenotype [32]. The importance of immunohistochemical study, including immunophenotyping, in secondary nodular liver lesions resulting from hematological malignancies lies in the possibility to differentially diagnose between reactive and neoplastic infiltrates, which cannot be accurately established by routine histological methods [33].

MM, similar to many malignancies, frequently results in significant changes in blood test parameters, especially after courses of chemotherapy and radiotherapy. Therefore, it is essential to emphasize that the patient, during the onset of COVID-19 and the rapid development of ARDS, had a hematologic malignancy, a condition which is considered a predictor of severe COVID-19 and a high risk of a fatal outcome [34]. According to Fattizzo *et al.*, increased mortality among patients with hematologic malignancies is primarily associated with increasing age and underlying health conditions [35]. In a study by He *et al.*, individuals admitted to hospital with bone marrow cancers had more severe disease course and higher infection-related mortality rate [36]. In the presented case, neutrophil left shift, elevated erythrocyte sedimentation rate, and lymphopenia exhibited comparable patterns during both the recurrence of multiple myeloma (MM), coinciding with the identification of secondary liver and root of the tongue involvement, and throughout the patient's course of COVID-19 (Table 1). The pathophysiology of neutrophil left shift in cancer is associated with the activation of granulopoiesis in the bone marrow by primary tumor, which stimulates the release and recruitment of neutrophils [37]. The latter, through interactions with lymphocytes, engage in both pro- and anti-tumor activities and can serve as biomarkers for disease progression and therapy response in cancer patients [37, 38]. The increased neutrophil-to-lymphocyte ratio observed in this case underscores the significant role of tumor-associated inflammation in cancer progression; it promotes malignant angiogenesis and is associated with worse survival [39]. The raised erythrocyte sedimentation rate in MM is an indirect marker of myeloma protein presence, leading to hypergammaglobulinemia, a phenomenon that accelerates falling of erythrocytes in a column [40] as a result of protein influence on the charge neutralizing sialic acid on the erythrocyte surface [41]. The patient exhibited comparable changes in the neutrophil-to-lymphocyte ratio and erythrocyte sedimentation rate during the episode of COVID-19 in November 2022, mirroring the alterations observed in the preceding MM recurrence a month earlier. It is essential to acknowledge that such changes are characteristic of acute viral infections as well. These laboratory data correlate with those by Feng at al. and Simadibrata *et al.*, who have concluded that high neutrophil-to-lymphocyte ratio can serve as a predictive marker for severe COVID-19 and rapid ARDS development [42, 43]. The erythrocyte sedimentation rate consistently remained elevated throughout the patient's medical history (Table 1), in contrast to the varying percentages of band and segmental neutrophils. Consequently, distinguishing the definitive and accurate cause of changes in laboratory parameters in patients who have undergone treatment for hematological malignancies poses a challenge [44, 45]. Severe COVID-19 can be associated with granulocytosis, as in the present case, as well as with granulocytopenia resulting from prolonged treatment of the underlying malignancy and leading to a higher susceptibility to bacterial co-infections during COVID-19 [36]. Frater *et al.* reported the correlation between lymphopenia, increased neutrophil count, and fatality in the general population, suggesting that anemia might play a crucial role in contributing to the hypoxic state and overall disease severity [46]. In the presented case, severe thrombocytopenia, a condition that is often caused by cytotoxic effect of bertezomib [47] and induced by radiation [48], was detected after chemo- and radiation therapy. Low platelet count, observed during readmission of our SARS-CoV-2-infected patient, is known to be associated with an increased risk of severe ARDS in adults and mortality from COVID-19 as well [49]. High serum urea and creatinine concentrations could be attributed to MM nephropathy [50] and/or nephrotoxic effect of chemotherapy [51]. Notably, hypercreatinemia and hyperuricemia observed in our patient during SARS-CoV-2 infection align with recent findings indicating their potential as predictors of severe outcomes in COVID-19, including acute kidney injury or in-hospital mortality [52]. Moreover, the presence of bacterial infections during the progression of COVID-19 has a notable influence on mortality in these individuals. It should be emphasized the potential for atypical clinical presentations and radiological manifestations in patients with bone marrow cancer, as the treatment of the underlying disease can modify the immune system response. This can potentially lead to delayed diagnosis of COVID-19, especially when swab tests yield negative test results [35]. Currently, our understanding of the impact of COVID-19 on MM patients remains incomplete and needs further research to investigate the association between MM-related immunosuppression and the COVID-19 uncontrolled immune-inflammatory cascade in COVID-19 [53].

From this case report, it is evident that the patient succumbed to death due to ARDS, spending a total of five days in the hospital from the onset of COVID-19 symptoms to his death. Despite intensive oxygen support, his condition progressively worsened, leading to increasing respiratory failure and ultimately resulting in a fatal outcome. The postmortem morphological findings were typical for diffuse alveolar damage characteristic of ARDS.

This is consistent with findings from a series of case reports where, among five MM patients with COVID-19, three individuals died due to progressive hypoxemic respiratory failure and one patient developed ARDS following temporary improvement [54]. ARDS is known to develop secondary to MM itself, characterized by diffuse alveolar infiltration by atypical plasma cells [55]. This is preceded by a gradual increase in respiratory failure due to diffuse alveolar metastatic calcification of the alveolar walls and blood vessels, accumulation of alveolar paraproteins, and amyloidosis of alveolar septa [56]. In the context of COVID-19, ARDS is induced by a cytokine storm, triggering an abnormal immune response marked by endothelial inflammation, vascular thrombosis, pulmonary infiltration, interstitial edema, and disruption of alveolar homeostasis, ultimately causing diffuse alveolar damage [57, 58]. In our case, morphological findings characteristic of ARDS in COVID-19 were found in the lung tissue at autopsy.

Conclusions

This case report aimed to document secondary liver involvement in MM, a relatively uncommon condition characterized by the formation of distinct metastatic nodules. These nodules exhibited hypo- and hyperechoic patterns on sonography and hypodensity during the venous phase of contrast-enhanced CT. Additionally, this clinical episode revealed the coexisting involvement of the tongue root secondary to MM, characterized by infiltration by atypical plasma cells. The second aspect was presenting a comprehensive clinical and laboratory profile, along with post-mortem findings, in a patient with concurrent COVID-19 and underlying MM, that may lead to development of ARDS and pose diagnostic challenges.

Ethical Statement

All study stages were performed in compliance with the principles of the Declaration of Helsinki and approved by the Ethics Committee of Ivano-Frankivsk National Medical University (Protocol No. 116/20 of October 07, 2020).

Informed Consent

Lifetime studies were conducted according to the informed consent of the patient, while postmortem studies were carried out in accordance with the informed consent of the legal representative of the deceased person, and included anonymity, confidentiality, voluntary participation, and the option to refuse participation in the study.

Acknowledgements

We thank the Department of Pathology of “Regional Clinical Hospital of Ivano-Frankivsk Regional Council” for support in histological image registration.

Data Availability

The anamnestic clinical, laboratory, radiological, and morphological data and images are available from the corresponding author. It is important to acknowledge the prohibition on transfers of personal data to third parties who did not participate in the study according to the conditions of informed consent signed by the legal representative of the deceased patient.

Conflict of Interest

The authors declare that no conflicts exist.

Financial Disclosure

This research was conducted without financial support.

References

[1] Kelley JT, Fuller LD, Lai KK, Yantiss RK, Dzedzik S, Alapat D, et al. Gastrointestinal, hepatic, and pancreatobiliary involvement by plasma cell neoplasms: clinicopathologic correlations in a retrospective cohort of 116 cases. Histopathology. 2022;81(6):742–757. Available from: https://doi.org/10.1111/his.14778

[2] Birjawi GA, Jalbout R, Musallam KM, Tawil AN, Taher AT, Khoury NJ. Abdominal manifestations of multiple myeloma: a retrospective radiologic overview. Clinical Lymphoma and Myeloma. 2008;8(6):348–351. Available from: https://doi.org/10.3816/CLM.2008.n.050

[3] Cho R, Myers DT, Onwubiko IN, Williams TR. Extraosseous multiple myeloma: imaging spectrum in the abdomen and pelvis. Abdominal Radiology. 2020;46(3):1194–1209. Available from: https://doi.org/10.1007/s00261-020-02712-2

[4] Bourdoncle S, Eche T, McGale J, Yiu K, Partouche E, Yeh R, et al. Investigating of the role of CT scan for cancer patients during the first wave of COVID-19 pandemic. Research in Diagnostic and Interventional Imaging. 2022;1:100004. Available from: https://doi.org/10.1016/j.redii.2022.100004

[5] Czernin J, Fanti S, Meyer PT, Allen-Auerbach M, Hacker M, Sathekge M, et al. Nuclear medicine operations in the times of COVID-19: strategies, precautions, and experiences. Journal of Nuclear Medicine. 2020;61(5):626–629. Available from: https://doi.org/10.2967/jnumed.120.245738

[6] Pagano L, Salmanton-García J, Marchesi F, et al. COVID-19 infection in adult patients with hematological malignancies: a European Hematology Association Survey (EPICOVIDEHA). Journal of Hematology & Oncology. 2021;14:168. Available from: https://doi.org/10.1186/s13045-021-01177-0

[7] Kamyshnyi A, Krynytska I, Matskevych V, Marushchak M, Lushchak O. Arterial hypertension as a risk comorbidity associated with COVID-19 pathology. International Journal of Hypertension. 2020;2020:8019360. Available from: https://doi.org/10.1155/2020/8019360

[8] Yang L, Chai P, Yu J, Fan X. Effects of cancer on patients with COVID-19: a systematic review and meta-analysis of 63,019 participants. Cancer Biology and Medicine. 2021;18(1):298–307. Available from: https://doi.org/10.20892/j.issn.2095-3941.2020.0559

[9] Kobilnyk Y, Mytsyk Y, Borzhievsky A, Vorobets D, Matskevych V. Dynamics of prostate cancer rate and mortality in Ukraine: current state of affairs. Proceedings of the Shevchenko Scientific Society Medical Sciences. 2020;62(2):06. Available from: https://doi.org/10.25040/ntsh2020.02.06

[10] Oh SM, Skendelas JP, Macdonald E, Bergamini M, Goel S, Choi J, et al. On-admission anemia predicts mortality in COVID-19 patients: a single center, retrospective cohort study. The American Journal of Emergency Medicine. 2021;48:140–147. Available from: https://doi.org/10.1016/j.ajem.2021.03.083

[11] Gaur N, Jha M, Tak M, Gupta R, Sharma P, Rajpurohit V, et al. Relationship of anemia with COVID-19 deaths: a retrospective cross-sectional study. Journal of Anaesthesiology Clinical Pharmacology. 2022;38(5):115. Available from: https://doi.org/10.4103/joacp.joacp_63_22

[12] Wang Y, Nan L, Hu M, Zhang R, Hao Y, Wang Y, et al. Significant association between anemia and higher risk for COVID-19 mortality: a meta-analysis of adjusted effect estimates. The American Journal of Emergency Medicine. 2022;58:281–285. Available from: https://doi.org/10.1016/j.ajem.2022.06.030

[13] Ludwig H, Sonneveld P, Facon T, San-Miguel J, Avet-Loiseau H, Mohty M, et al. COVID-19 vaccination in patients with multiple myeloma: a consensus of the European Myeloma Network. The Lancet Haematology. 2021;8(12):e934–e46. Available from: https://doi.org/10.1016/S2352-3026(21)00278-7

[14] Prokop M, van Everdingen W, van Rees Vellinga T, Quarles van Ufford H, Stöger L, Beenen L, et al. CO-RADS: a categorical CT assessment scheme for patients suspected of having COVID-19—definition and evaluation. Radiology. 2020;296(2):E97–E104. Available from: https://doi.org/10.1148/radiol.2020201473

[15] Wu XN, Zhao XY, Jia JD. Nodular liver lesions involving multiple myeloma: a case report and literature review. World Journal of Gastroenterology. 2009;15(8):1014–1017. Available from: https://doi.org/10.3748/wjg.15.1014

[16] Oshima K, Kanda Y, Nannya Y, Kaneko M, Hamaki T, Suguro M, et al. Clinical and pathologic findings in 52 consecutively autopsied cases with multiple myeloma. American Journal of Hematology. 2001;67(1):1–5. Available from: https://doi.org/10.1002/ajh.1067

[17] Heckmann M, Uder M, Grgic A, Adrian N, Bautz W, Heinrich M. Extraosseous manifestation of multiple myeloma with unusual appearance in computed tomography – case report. Rontgenpraxis. 2008;56(6):249–253. Available from: https://doi.org/10.1016/j.rontge.2008.03.003

[18] Talamo G, Cavallo F, Zangari M, Barlogie B, Lee CK, Pineda-Roman M, Kiwan E, Krishna S, Tricot G. Clinical and biological features of multiple myeloma involving the gastrointestinal system. Haematologica. 2006;91:964–967.

[19] Kwok H, Lo ES, Wong T, Lee HH, Chau H, Ng F, et al. Extraosseous myeloma of liver mimicking multifocal hepatocellular carcinoma where a distinction has to be made: two case reports. Hong Kong Medical Journal. 2023;29(1):66–69. Available from: https://doi.org/10.12809/hkmj219640

[20] Lu YY, Chen JH, Lin WY, Liang JA, Wang HY, Tsai SC, et al. FDG PET or PET/CT for detecting intramedullary and extramedullary lesions in multiple myeloma. Clinical Nuclear Medicine. 2012;37(9):833–7. Available from: https://doi.org/10.1097/RLU.0b013e31825b2071

[21] Chakraborty R, Hillengass J, Lentzsch S. How do we image patients with multiple myeloma and precursor states? British Journal of Haematology. 2023;203(4):536–545. Available from: https://doi.org/10.1111/bjh.18880

[22] Gariani J, Westerland O, Natas S, Verma H, Cook G, Goh V. Comparison of whole body magnetic resonance imaging (WBMRI) to whole body computed tomography (WBCT) or 18 F-fluorodeoxyglucose positron emission tomography/CT (18 F-FDG PET/CT) in patients with myeloma: aystematic review of diagnostic performance. Critical Reviews in Oncology/Hematology. 2018;124:66–72. Available from: https://doi.org/10.1016/j.critrevonc.2018.02.012

[23] Rama S, Suh CH, Kim KW, Durieux JC, Ramaiya NH, Tirumani SH. Comparative performance of whole-body MRI and FDG PET/CT in evaluation of multiple myeloma treatment response: systematic review and meta-analysis. American Journal of Roentgenology. 2022;218(4):602–613. Available from: https://doi.org/10.2214/AJR.21.26381

[24] Yokoyama K, Tsuchiya J, Tateishi U. Comparison of [18F]FDG PET/CT and MRI for Treatment Response Assessment in Multiple Myeloma: A Meta-Analysis. Diagnostics. 2021;11(4):706. Available from: https://doi.org/10.3390/diagnostics11040706

[25] Erdoğan YE, Yavuz B, Karataş AF, Alacacıoğlu İ, Özkal S, Diçle O, et al. Liver plasmacytoma mimicking solid tumor metastasis in a relapsed myeloma patient: case report and review of the literature. İzmir Tıp Fakültesi Dergisi. 2022;1(2):103–106.

[26] Hillengass J, Landgren O. Challenges and opportunities of novel imaging techniques in monoclonal plasma cell disorders: imaging "early myeloma." Leukemia & Lymphoma. 2013;54(7):1355–1363. Available from: https://doi.org/10.3109/10428194.2012.740559

[27] Rajkumar SV. Multiple myeloma: 2022 update on diagnosis, risk stratification, and management. American Journal of Hematology. 2022;97(8):1086–1107. Available from: https://doi.org/10.1002/ajh.26590

[28] Xing Y, Qiu J, Zhou ML, Zhou SH, Bao YY, Wang QY, et al. Prognostic factors of laryngeal solitary extramedullary plasmacytoma: a case report and review of literature. Internal Journal of Clinical and Experimental Pathology. 2015;8(3):2415–2435.

[29] Alexiou C, Kau RJ, Dietzfelbinger H, Kremer M, Spiess JC, Schratzenstaller B, et al. Extramedullary plasmacytoma. Cancer. 1999;85(11):2305–2314. Available from: https://doi.org/10.1002/(SICI)1097-0142(19990601)85:11¡2305::AID-CNCR2¿3.0.CO;2-3

[30] Berdica L, Bushati T, Aga A, Vajushi E, Sukaj E, Ndoja A, et al. Extramedullary plasmacytoma of the tongue: a case report. Journal of Clinical Images and Medical Case Reports. 2021;2(6):1409. Available from: https://doi.org/10.52768/2766-7820/1409

[31] Ramalingam P, Adeagbo B, Bollag R, Lee J, Reid-Nicholson M. Metastatic hepatocellular carcinoma with CD138 positivity: an unusual mimic of multiple myeloma? Diagnostic Cytopathology. 2008;36(10):742–748. Available from: https://doi.org/10.1002/dc.20888

[32] Pizzi M, Sbaraglia M, Dal Santo L, De Bartolo D, Santoro L, Scarmozzino F, et al. Higher accuracy of surgical over core needle biopsy for the diagnosis of lymphoproliferative disorders. International Journal of Laboratory Hematology. 2023;45(4):516–521. Available from: https://doi.org/10.1111/ijlh.14055

[33] Walz-Mattmüller R, Horny HP, Ruck P, Kaiserling E. Incidence and pattern of liver involvement in haematological malignancies. Pathology - Research and Practice. 1998;194(11):781–789. Available from: https://doi.org/10.1016/S0344-0338(98)80068-X

[34] Vijenthira A, Gong IY, Fox TA, Booth S, Cook G, Fattizzo B, et al. Outcomes of patients with hematologic malignancies and COVID-19: a systematic review and meta-analysis of 3377 patients. Blood. 2020;136(25):2881–2892. Available from: https://doi.org/10.1182/blood.2020008824

[35] Fattizzo B, Giannotta JA, Sciumè M, Cattaneo D, Bucelli C, Fracchiolla NS, et al. Reply to "COVID-19 in persons with haematological cancers": a focus on myeloid neoplasms and risk factors for mortality. Leukemia. 2020;34(7):1957–1960. Available from: https://doi.org/10.1038/s41375-020-0877-y

[36] He W, Chen L, Chen L, Yuan G, Fang Y, Chen W, et al. COVID-19 in persons with haematological cancers. Leukemia. 2020;34(6):1637–1645. Available from: https://doi.org/10.1038/s41375-020-0836-7

[37] Coffelt SB, Wellenstein MD, de Visser KE. Neutrophils in cancer: neutral no more. Nature Reviews Cancer. 2016;16(7):431–446. Available from: https://doi.org/10.1038/nrc.2016.52

[38] Chrysanthakopoulos NA, Vryzaki E. Anticancer agent effect and polychemotherapy regimens for malignant tumor treatment - a review. Galician Medical Journal. 2022;29(2):E202227. Available from: https://doi.org/10.21802/gmj.2022.2.7

[39] Aganović-Mušinović I, Sofo-Hafizović A, RakanovćTodić M, Maleškić Kapo S, Mahmutović-Vranić S, Mačkić-Durović M, et al. Evaluation of the neutrophil to lymphocyte ratio and monocyte to lymphocyte ratio in patients with multiple myeloma. International Journal of Medical Science and Dental Research. 2023;6(2):48–55. Available from: https://www.ijmsdr.org/published%20paper/1i1i27/evaluation-of-the-neutrophil-to-lymphocyte-ratio-and-monocyte-to-lymphocyte-ratio-in-patients-with-multiple-myeloma.pdf

[40] Harrison M. Abnormal laboratory results: erythrocyte sedimentation rate and C-reactive protein. Australian Prescriber. 2015;38(3):93–94. Available from: https://doi.org/10.18773/austprescr.2015.034

[41] Firth J, CME Medical Masterclass. Haematology: multiple myeloma. Clinical Medicine. 2019;19(1):58–60. Available from: https://doi.org/10.7861/clinmedicine.19-1-58

[42] Feng X, Li S, Sun Q, Zhu J, Chen B, Xiong M, et al. Immune-inflammatory parameters in COVID-19 cases: a systematic review and meta-analysis. Frontiers in Medicine. 2020;7:301. Available from: https://doi.org/10.3389/fmed.2020.00301

[43] Simadibrata DM, Calvin J, Wijaya AD, Ibrahim NAA. Neutrophil-to-lymphocyte ratio on admission to predict the severity and mortality of COVID-19 patients: a meta-analysis. The American Journal of Emergency Medicine. 2021;42:60–69. Available from: https://doi.org/10.1016/j.ajem.2021.01.006

[44] Skakun O, Fedorov S, Seredyuk N, Verbovska O. Prognostic value of serum Interleukin-6 level in hypertensive patients with COVID-19-Associated pneumonia. Galician Medical Journal. 2022;29(4):E202242. Available from: https://doi.org/10.21802/gmj.2022.4.2

[45] Kindrativ EO, Vasylyk VM, Matskevych VM, Kostyuk VM, Semchenko VA, Voronych VO. Retrospective analysis of coronavirus disease lethal cases. Fiziolohichnyĭ zhurnal. 2021;67(4):76–85. Available from: https://doi.org/10.15407/fz67.04.076

[46] Frater JL, Zini G, d'Onofrio G, Rogers HJ. COVID-19 and the clinical hematology laboratory. International Journal of Laboratory Hematology. 2020;42(S1):11–18. Available from: https://doi.org/10.1111/ijlh.13229

[47] Lonial S, Waller EK, Richardson PG, Jagannath S, Orlowski RZ, Giver CR, et al. Risk factors and kinetics of thrombocytopenia associated with bortezomib for relapsed, refractory multiple myeloma. Blood. 2005;106(12):3777–3784. Available from: https://doi.org/10.1182/blood-2005-03-1173

[48] Satheesh Kumar P, Balan A, Sankar A, Bose T. Radiation induced oral mucositis. Indian Journal of Palliative Care. 2009;15(2):95. Available from: https://doi.org/10.4103/0973-1075.58452

[49] Lippi G, Plebani M, Henry BM. Thrombocytopenia is associated with severe coronavirus disease 2019 (COVID-19) infections: a meta-analysis. Clinica Chimica Acta. 2020;506:145–148. Available from: https://doi.org/10.1016/j.cca.2020.03.022

[50] Yadav P, Cook M, Cockwell P. Current trends of renal impairment in multiple myeloma. Kidney Diseases. 2015;1(4):241–257. Available from: https://doi.org/10.1159/000442511

[51] Drayson M, Begum G, Basu S, Makkuni S, Dunn J, Barth N, et al. Effects of paraprotein heavy and light chain types and free light chain load on survival in myeloma: an analysis of patients receiving conventional-dose chemotherapy in Medical Research Council UK multiple myeloma trials. Blood. 2006;108(6):2013–2019. Available from: https://doi.org/10.1182/blood-2006-03-008953

[52] Cheng Y, Luo R, Wang K, Zhang M, Wang Z, Dong L, et al. Kidney disease is associated with in-hospital death of patients with COVID-19. Kidney International. 2020;97(5):829–838. Available from: https://doi.org/10.1016/j.kint.2020.03.005

[53] Wang B, Van Oekelen O, Mouhieddine TH, Del Valle DM, Richter J, Cho HJ, et al. A tertiary center experience of multiple myeloma patients with COVID-19: lessons learned and the path forward. Journal of Hematology & Oncology. 2020;13(1):94. Available from: https://doi.org/10.1186/s13045-020-00934-x

[54] Dhakal B, D'Souza A, Chhabra S, Hari P. Multiple myeloma and COVID-19. Leukemia. 2020;34(7):1961–1963. Available from: https://doi.org/10.1038/s41375-020-0879-9

[55] Al-Kuraishy HM, Al-Gareeb AI, Mohammed AA, Alexiou A, Papadakis M, Batiha GE. The potential link between Covid-19 and multiple myeloma: A new saga. Immunity, Inflammation and Disease. 2022;10(12):e701. Available from: https://doi.org/10.1002/iid3.701

[56] Marmor DB. Acute respiratory distress syndrome due to pulmonary involvement by neoplastic plasma cells in multiple myeloma. Thorax. 2006;61(5):455–456. Available from: https://doi.org/10.1136/thx.2004.029397

[57] Matskevych V, Kamyshnyi O, Vasylyk VM, Grynovska MB, Lenchuk T, Fishchuk R, et al. Morphological prediction of lethal outcomes in the evaluation of lung tissue structural changes in patients on respiratory support with COVID-19: Ukrainian experience. Pathology - Research and Practice. 2023;245:154471. Available from: https://doi.org/10.1016/j.prp.2023.154471

[58] Perlin DS, Neil GA, Anderson C, Zafir-Lavie I, Raines S, Ware CF, et al. Randomized, double-blind, controlled trial of human anti-LIGHT monoclonal antibody in COVID-19 acute respiratory distress syndrome. Journal of Clinical Investigation. 2022;132(3):e153173. Available from: https://doi.org/10.1172/JCI153173